Vector–axial-vector mixing from a chiral effective field theory at finite temperature

Masayasu Harada,[1] Chihiro Sasaki,[2] and Wolfram Weise[2]

[1]*Department of Physics, Nagoya University, Nagoya, 464-8602, Japan*
[2]*Physik-Department, Technische Universität München, D-85747 Garching, Germany*

We study the vector–axial-vector mixing in a hot medium and its evolution toward the chiral phase transition using different symmetry restoration scenarios based on the generalized hidden local symmetry framework. We show that the presence of the a_1 meson reduces the vector spectral function around the ρ meson mass and enhances it around the a_1 meson mass. The coupling strength of a_1 to ρ and π vanishes at the critical temperature due to the degenerate ρ-a_1 masses. This feature holds rigorously in the chiral limit and still stays intact to good approximation for the physical pion mass.

I. INTRODUCTION

In-medium changes of hadron properties are considered to be indicators of the tendency towards chiral symmetry restoration in hot and/or dense QCD. In particular, the short-lived vector mesons like the ρ mesons are expected to carry information on the modifications of hadrons in matter [1]. In the presence of hot matter the vector and axial-vector current correlators are mixed due to pions in the heat bath. At low temperatures this process is described in a model-independent way in terms of a low-energy theorem based on chiral symmetry [2]. The vector spectral function is then modified by axial-vector mesons through the mixing theorem [3].

The validity of this theorem is, however, limited to temperatures $T \ll 2f_\pi$, where f_π is the pion decay constant in vacuum. At higher temperatures hadrons other than pions are thermally activated. Thus one needs in-medium correlators systematically involving those excitations.

In this paper we show the effects of the mixing (hereafter V-A mixing), and how the axial-vector mesons affect the spectral function near the chiral phase transition, within an effective field theory. Our analysis will be carried out assuming several possible patterns of chiral symmetry restoration: dropping or nondropping ρ meson mass along with changing a_1 meson mass, both considered to be options from a phenomenological point of view. The effect of explicit chiral symmetry breaking is also examined.

II. GENERALIZED HIDDEN LOCAL SYMMETRY

Several models exist which explicitly include the axial-vector meson in addition to the pion and vector meson consistently with the chiral symmetry of QCD, such as the massive Yang-Mills model [4], the antisymmetric tensor field method [5] and the approach based on generalized hidden local symmetry (GHLS) [6,7]. These models are equivalent [7–9] for tree-level amplitudes in the low-energy limit.

A. Lagrangian

The GHLS Lagrangian is based on a $G_{\mathrm{global}} \times G_{\mathrm{local}}$ symmetry, where $G_{\mathrm{global}} = [SU(N_f)_L \times SU(N_f)_R]_{\mathrm{global}}$ is the chiral symmetry and $G_{\mathrm{local}} = [SU(N_f)_L \times SU(N_f)_R]_{\mathrm{local}}$ is the GHLS. The whole symmetry $G_{\mathrm{global}} \times G_{\mathrm{local}}$ is spontaneously broken to a diagonal $SU(N_f)_V$. The basic quantities are the GHLS gauge bosons, L_μ and R_μ, identified with the vector and axial-vector mesons as $V_\mu = (R_\mu + L_\mu)/2$ and $A_\mu = (R_\mu - L_\mu)/2$, and three matrix valued variables ξ_L, ξ_R, and ξ_M, which are combined in an $N_f \times N_f$ special-unitary matrix $U = \xi_L^\dagger \xi_M \xi_R$.

The fundamental objects are the Maurer-Cartan one-forms defined by

$$\hat{\alpha}_{L,R}^\mu = D^\mu \xi_{L,R} \cdot \xi_{L,R}^\dagger / i, \qquad \hat{\alpha}_M^\mu = D^\mu \xi_M \cdot \xi_M^\dagger / (2i), \tag{2.1}$$

where the covariant derivatives of $\xi_{L,R,M}$ are given by

$$\begin{aligned}
D_\mu \xi_L &= \partial_\mu \xi_L - iL_\mu \xi_L + i\xi_L \mathcal{L}_\mu, \\
D_\mu \xi_R &= \partial_\mu \xi_R - iR_\mu \xi_R + i\xi_R \mathcal{R}_\mu, \\
D_\mu \xi_M &= \partial_\mu \xi_M - iL_\mu \xi_M + i\xi_M R_\mu,
\end{aligned} \tag{2.2}$$

with $\mathcal{L}_\mu$ and $\mathcal{R}_\mu$ being the external gauge fields introduced by gauging G_{global}. There are four independent terms with lowest derivatives:

$$\begin{aligned}
\mathcal{L}_V &= F^2 \, \mathrm{tr}[\hat{\alpha}_{\parallel\mu} \hat{\alpha}_\parallel^\mu], \\
\mathcal{L}_A &= F^2 \, \mathrm{tr}[\hat{\alpha}_{\perp\mu} \hat{\alpha}_\perp^\mu], \\
\mathcal{L}_M &= F^2 \, \mathrm{tr}[\hat{\alpha}_{M\mu} \hat{\alpha}_M^\mu], \\
\mathcal{L}_\pi &= F^2 \, \mathrm{tr}[(\hat{\alpha}_{\perp\mu} + \hat{\alpha}_{M\mu})(\hat{\alpha}_\perp^\mu + \hat{\alpha}_M^\mu)],
\end{aligned} \tag{2.3}$$

where F is a parameter of dimension 1 and $\hat{\alpha}_{\parallel,\perp}^\mu = (\xi_M \hat{\alpha}_R^\mu \xi_M^\dagger \pm \hat{\alpha}_L^\mu)/2$. The kinetic term of the gauge bosons is given by

$$\mathcal{L}_{\text{kin}}(L_\mu, R_\mu) = -\frac{1}{4g^2}\,\text{tr}[L_{\mu\nu}L^{\mu\nu} + R_{\mu\nu}R^{\mu\nu}], \quad (2.4)$$

where g is the GHLS gauge coupling and the field strengths are defined by $L_{\mu\nu} = \partial_\mu L_\nu - \partial_\nu L_\mu - i[L_\mu, L_\nu]$ and $R_{\mu\nu} = \partial_\mu R_\nu - \partial_\nu R_\mu - i[R_\mu, R_\nu]$.

Combining the terms (2.3) and (2.4), the GHLS Lagrangian is given by

$$\mathcal{L} = a\mathcal{L}_V + b\mathcal{L}_A + c\mathcal{L}_M + d\mathcal{L}_\pi + \mathcal{L}_{\text{kin}}(L_\mu, R_\mu), \quad (2.5)$$

where a, b, c, and d are dimensionless parameters. Fields for three types of Nambu-Goldstone bosons, ϕ_σ, $\phi_\perp$ and ϕ_p, are introduced as

$$\xi_{L,R} = e^{i(\phi_\sigma \mp \phi_\perp)}, \qquad \xi_M = e^{2i\phi_p}. \quad (2.6)$$

The pion field ϕ_π is given by the combination

$$\phi_\pi = \phi_\perp + \phi_p, \quad (2.7)$$

while two remaining would-be Nambu-Goldstone bosons [10], ϕ_σ and

$$\phi_q = \frac{1}{b+c}(c\phi_p - b\phi_\perp), \quad (2.8)$$

representing the longitudinal vector and axial-vector degrees of freedom, are absorbed into the ρ and a_1. The π, σ, and q fields are normalized by corresponding decay constants:

$$\phi_\pi = \frac{\pi}{F_\pi}, \qquad \phi_\sigma = \frac{\sigma}{F_\sigma}, \qquad \phi_q = \frac{q}{F_q}. \quad (2.9)$$

The pion decay constant, the meson bare masses, and the coupling strength of the ρ and a_1 to the vector and axial-vector currents, J^μ and J_5^μ, are given by

$$F_\pi^2 = \left(d + \frac{bc}{b+c}\right)F^2, \qquad M_\rho^2 = g^2 F_\sigma^2 = ag^2 F^2,$$

$$M_{a_1}^2 = g^2 F_q^2 = (b+c)g^2 F^2, \qquad g_\rho = agF^2,$$

$$g_{a_1} = bgF^2. \quad (2.10)$$

B. Weinberg sum rules

The axial-vector and vector current correlators are defined as

$$\int d^4 x e^{iqx}\langle 0|TJ_5^\mu(x)J_5^\nu(0)|0\rangle = G_A(Q^2)(q^\mu q^\nu - q^2 g^{\mu\nu}),$$

$$\int d^4 x e^{iqx}\langle 0|TJ^\mu(x)J^\nu(0)|0\rangle = G_V(Q^2)(q^\mu q^\nu - q^2 g^{\mu\nu}),$$

$$(2.11)$$

where $Q^2 = -q^2 > 0$ is the spacelike squared momentum. When these correlators are saturated by the lowest lying mesons at tree level, we have

$$G_A(Q^2) = \frac{F_\pi^2}{Q^2} + \frac{F_{a_1}^2}{M_{a_1}^2 + Q^2}, \qquad G_V(Q^2) = \frac{F_\rho^2}{M_\rho^2 + Q^2}, \quad (2.12)$$

where the a_1 and ρ decay constants are defined by

$$F_{a_1}^2 = \left(\frac{g_{a_1}}{M_{a_1}}\right)^2 = \frac{b^2}{b+c}F^2, \qquad F_\rho^2 = \left(\frac{g_\rho}{M_\rho}\right)^2 = aF^2. \quad (2.13)$$

The same correlators can be evaluated by the operator product expansion (OPE), which shows that the difference between two correlators scales as $1/Q^6$ [11][1]:

$$G_A^{(\text{OPE})}(Q^2) - G_V^{(\text{OPE})}(Q^2) = \frac{32\pi}{9}\frac{\alpha_s\langle\bar{q}q\rangle^2}{Q^6}. \quad (2.14)$$

We require that the high-energy behavior of the difference between the two correlators in the GHLS agrees with that in the OPE: $G_A(Q^2) - G_V(Q^2)$ approaches $\sim 1/Q^6$. This condition is satisfied only if the following relations hold:

$$F_\pi^2 + F_{a_1}^2 = F_\rho^2, \qquad F_{a_1}^2 M_{a_1}^2 = F_\rho^2 M_\rho^2, \quad (2.15)$$

which are nothing but the pole saturated forms of the Weinberg first and second sum rules [12]. In terms of the parameters of the GHLS Lagrangian, the above relations can be traced back to

$$a = b, \qquad d = 0. \quad (2.16)$$

In Ref. [10] it was shown that the parameter relations are stable against the renormalization group evolution: This implies *the nonrenormalization of the Weinberg sum rules expressed in terms of the leading order parameters in the GHLS.*[2] In the following studies, we adopt the GHLS Lagrangian with $a = b$ and $d = 0$ as a reliable basis which describes the spectral function sum rules.

C. Explicit chiral symmetry breaking

Explicit chiral symmetry breaking due to the current quark masses is introduced through

$$\hat{\chi} = 2B\xi_L \mathcal{M}\xi_R^\dagger, \quad (2.17)$$

where $\mathcal{M}$ is the quark mass matrix and B is a constant with dimension 1. The transformation property under the chiral symmetry is

$$\hat{\chi} \to h_L \hat{\chi} h_R, \quad (2.18)$$

where $h_{L,R} \in [\text{SU}(N_f)_{L,R}]_{\text{local}}$. Symmetry breaking terms

---

[1]We assume factorization of four-quark condensates.
[2]The GHLS Lagrangian does not include scalar $\bar{q}q$ modes which are assumed to be heavier than other mesons incorporated. This may not be true near the critical point within the Ginzburg-Landau picture of the phase transition. The scalar mesons thus modify the renormalization group structure.

TABLE I.   Upper line: input quantities taken from PDG [13]. The values of g_ρ and $g_{\rho\pi\pi}$ are estimated from the decay widths $\Gamma(\rho \to e^+e^-)$ and $\Gamma(\rho \to \pi\pi)$. Lower line: resulting model parameters.

F_π [GeV]	m_π [GeV]	m_K [GeV]	M_ρ [GeV]	M_{K^*} [GeV]	M_{a_1} [GeV]	$M_{K_{1A}}$ [GeV]	g_ρ [GeV^2]	$g_{\rho\pi\pi}$
0.0924	0.140	0.494	0.775	0.892	1.26	1.34	0.119	6.00

aF^2 [GeV^2]	cF^2 [GeV^2]	g	h_V	h_A	$z_\rho \times 10^3$	$z_{\rho\pi\pi} \times 10^3$		
0.0133	0.0226	6.61	0.869	0.927	−7.09	−6.21		

relevant to the meson masses are found as[3]

$$\mathcal{L}_{\chi SB} = \frac{h_V}{g^2} \, \text{tr}[(\hat{\alpha}_\parallel^\mu \hat{\alpha}_{\parallel\mu} + \hat{\alpha}_\perp^\mu \hat{\alpha}_{\perp\mu})(\hat{\chi}\xi_M^\dagger + \xi_M\hat{\chi}^\dagger)]$$
$$+ \frac{h_A - h_V}{g^2} \, \text{tr}[\hat{\alpha}_M^\mu \hat{\alpha}_{M\mu}(\hat{\chi}\xi_M^\dagger + \xi_M\hat{\chi}^\dagger)],$$

(2.19)

with coefficients h_V and h_A. The additional piece (2.19) in the Lagrangian gives the meson masses and the pion decay constant as

$$M_\rho^2 = ag^2F^2 + h_V m_\pi^2, \qquad M_{a_1}^2 = (a + c)g^2F^2 + h_A m_\pi^2,$$
$$F_\pi^2 = \left(cF^2 + \frac{h_A - h_V}{g^2}m_\pi^2\right)\frac{M_\rho^2}{M_{a_1}^2},$$

(2.20)

with nonzero pion mass m_π and to leading order in the symmetry breaking quark masses. Flavor symmetry leads to the following relations in terms of light nonstrange ($s = 0$) and strange meson masses

$$M_\rho^2 = ag^2F^2 + h_V m_\pi^2, \qquad M_{K^*}^2 = ag^2F^2 + h_V m_K^2.$$

(2.21)

One finds

$$h_V = \frac{M_{K^*}^2 - M_\rho^2}{m_K^2 - m_\pi^2}.$$

(2.22)

The isospin $\frac{1}{2}$ states with $J^{PC} = 1^{+\pm}$ are mixed. The $K_{1A}(1^{++})$ and $K_{1B}(1^{+-})$ are nearly equal mixtures of the $K_1(1270)$ and $K_1(1400)$ (with a 45° mixing angle) [13]. Thus, the h_A is expressed as

$$h_A = \frac{M_{K_{1A}}^2 - M_{a_1}^2}{m_K^2 - m_\pi^2}.$$

(2.23)

In the present model, the coupling of a_1 to ρ-π is determined by

$$g_{a_1\rho\pi} = -g^2 F_\pi,$$

(2.24)

where F_π is given in Eq. (2.20). For expressing the ρ-photon mixing strength g_ρ and ρ-π-π coupling $g_{\rho\pi\pi}$

---

[3]In general, there are six independent terms including the two of $\hat{\alpha}_{\parallel,\perp}$ and $\hat{\alpha}_M$ in one trace. Here we use two terms which contribute to the masses of vector and axial-vector mesons. Furthermore, we neglect the correction to the kinetic term of the gauge fields.

we introduce the higher derivative terms [9,14]. The resultant expressions are given by

$$g_\rho(s) = g\left(aF^2 + \frac{h_V}{g^2}m_\pi^2 - z_\rho s\right),$$
$$g_{\rho\pi\pi}(s) = \frac{g}{2}\left(1 + \frac{M_\rho^2}{M_{a_1}^2} - z_{\rho\pi\pi}\frac{s}{F_\pi^2}\right),$$

(2.25)

with the squared four-momentum $s = p^2$ and dimensionless constants z_ρ and $z_{\rho\pi\pi}$. The parameters are fixed by comparison with experimental values listed in Table I.

III. CHIRAL SYMMETRY RESTORATION

The critical temperature T_c for the restoration of chiral symmetry in its Wigner-Weyl realization is defined as the temperature at which the vector and axial-vector current correlators coincide and their spectra become degenerate. Expanding the correlators (2.12) in the meson rest frame, one finds

$$G_A - G_V \propto M_\rho^2(M_{a_1}^2 - M_\rho^2) = M_\rho^2 \delta M^2.$$

(3.1)

Then chiral symmetry restoration implies either $\delta M = 0$ or $M_\rho = 0$ (or both) at $T = T_c$: Either the ρ-a_1 mass difference δM or the ρ meson mass is identified as a measure of spontaneous chiral symmetry breaking and acts as an order parameter of the chiral phase transition.

A. Option A: dropping a_1 and nondropping ρ masses

The GHLS theory describes the chiral symmetry restoration with massless ρ and a_1 mesons in the chiral limit [10] (see also next subsection). The classification of possible restoration patterns relies on the renormalization group equations (RGEs). The theory does not have explicit scalar $\bar{q}q$ modes which will be important in the vicinity of the critical temperature. The scalar bosons may modify the RGEs and the massless mesons, protected by the fixed point of the RGEs, might not necessarily be uniquely associated with the chiral symmetry restoration. This option suggests a symmetry restoration scenario in which nonvanishing ρ and a_1 masses become degenerate at $T = T_c$.

For the case of nondropping ρ mass, we will examine δM changing with temperature intrinsically such that $G_A - G_V = 0$ at the chiral transition. To achieve $G_A = G_V$ with $\delta M = 0$ at the critical temperature, we adopt the following ansatz of the temperature dependence of the *bare*

axial-vector meson mass:

$$M_{a_1}^2 = M_\rho^2 + \delta M^2(T), \qquad \delta M^2(T) = c(T)g^2 F^2, \quad (3.2)$$

with

$$c(T) = c\Theta(T_f - T) + c\Theta(T - T_f)\frac{T_c^2 - T^2}{T_c^2 - T_f^2}, \quad (3.3)$$

$$g(T) = g,$$

where we schematically introduce the "flash temperature" T_f [15] which controls how the mesons experience partial restoration of chiral symmetry. The temperature dependence of $c(T)$ as well as the critical temperature T_c are in principle determined by QCD, e.g. through the matching to the QCD current correlators of finite temperature. We adopt here a simplified parameterization of the T dependence[4] in which the values of T_c and T_f are taken in a reasonable range as indicated, for example, by the onset of the chiral crossover transition observed in lattice QCD [17]. We take $T_c = 200$ MeV and $T_f = 0.7T_c$ for our numerical calculations.

For finite m_π the temperature dependence of the a_1 meson mass is given by

$$M_{a_1}^2(T) = (a + c(T))g^2 F^2 + h_A m_\pi^2, \quad (3.4)$$

where m_π is assumed to be independent of temperature.

B. Option B: dropping a_1 and ρ masses

The phase structure of the GHLS theory in vacuum was studied in detail based on the RG flows at one loop [10] assuming that the scalar mesons are heavier than any other mesons and are integrated out near the critical point. Here we give a brief summary of the chiral symmetry restoration with massless ρ and a_1 mesons in the GHLS. In this case chiral symmetry restoration can be realized only if the gauge coupling vanishes at the critical point,

$$g \to 0, \quad (3.5)$$

when one requires the first and second Weinberg sum rules to be satisfied. This option leads to the ρ and a_1 mesons being massless:

$$M_\rho \to 0, \qquad M_{a_1} \to 0. \quad (3.6)$$

The vanishing masses are not renormalized at the critical point since $g = 0$ is the only fixed point of its RGE. This is a field theoretical description of the dropping masses following Brown-Rho scaling [18]. Possible patterns of the symmetry restoration are classified by the mass ratio

M_ρ/M_{a_1} which flows into one of the following fixed points[5]:

(I) $\rho - a_1$ chiral partners: $M_\rho^2/M_{a_1}^2 \to 1$,

(II) $\rho - \pi$ chiral partners: $M_\rho^2/M_{a_1}^2 \to 0$. $\quad$ (3.7)

These cases correspond to the Lagrangian parameters as

(I) $a \neq 0$, $\quad$ $c \to 0$, $\quad$ (II) $a \to 0$, $\quad$ $c \neq 0$. $\quad$ (3.8)

The dropping ρ and a_1 masses are described by the T-dependent gauge coupling $g(T)$ parameterized as [14]

$$g(T) = g\Theta(T_f - T) + g\Theta(T - T_f)\sqrt{\frac{T_c^2 - T^2}{T_c^2 - T_f^2}}. \quad (3.9)$$

Two possible cases of chiral symmetry restoration are thus distinguished by adopting the following parameterization with Eq. (3.9):

(I) : $a(T) = a$,

$$c(T) = c\Theta(T_f - T) + c\Theta(T - T_f)\frac{T_c^2 - T^2}{T_c^2 - T_f^2}, \quad (3.10)$$

(II) : $a(T) = a\Theta(T_f - T) + a\Theta(T - T_f)\frac{T_c^2 - T^2}{T_c^2 - T_f^2}$,

$$c(T) = c. \quad (3.11)$$

In the presence of explicit chiral symmetry breaking, the ρ and a_1 meson masses have the following temperature dependence:

(I) : $M_\rho^2(T) = ag^2(T)F^2 + h_V m_\pi^2$,

$$M_{a_1}^2(T) = (a + c(T))g^2(T)F^2 + h_A m_\pi^2, \quad (3.12)$$

(II) : $M_\rho^2(T) = a(T)g^2(T)F^2 + h_V m_\pi^2$,

$$M_{a_1}^2(T) = (a(T) + c)g^2(T)F^2 + h_A m_\pi^2, \quad (3.13)$$

with the scaling behaviors given in Eqs. (3.9), (3.10), and (3.11).

IV. VECTOR SPECTRAL FUNCTION

The vector current correlator Eq. (2.11) in GHLS is expressed in terms of two-point functions of the vector gauge field V^μ and the external field $\mathcal{V}^\mu$ as [19]

$$G_V = \frac{\Pi_V^S(\Pi_V^{LT} + 2\Pi_{V\|}^{LT})}{\Pi_V^S - \Pi_V^{LT}} + \Pi_\|^{LT}, \quad (4.1)$$

where Π_V, $\Pi_{V\|}$ and $\Pi_\|$ are V-V, V-$\mathcal{V}$, and $\mathcal{V}$-$\mathcal{V}$ corre-

---

[4]The pion decay constant near the critical temperature T_c behaves as $f_\pi^2 \sim T_c^2 - T^2$ in the chiral limit [16]. The parameterization in Eq. (3.3) describes this scaling. Here the F_π denotes the tree-level parameter given in Eq. (2.10), while the f_π indicates the physical quantity including hadronic corrections which are generated from loop diagrams at finite temperature.

[5]Besides (I) and (II), the fixed point $M_\rho^2/M_{a_1}^2 \to 1/3$ also leads to a possible restoration pattern [10]. This is an ultraviolet fixed point in any direction, so that it is not stable as to (I) and (II). Thus, we will consider only type (I) and (II) in this paper.

lation functions given explicitly in the appendix, with the following generic tensor decomposition:

$$\Pi^{\mu\nu} = g^{\mu\nu}\Pi^S + \left(\frac{q^\mu q^\nu}{q^2} - g^{\mu\nu}\right)\Pi^{LT}. \qquad (4.2)$$

The vector spectral function is defined as the imaginary part of the vector correlator in Eq. (4.1).

A. Option A: dropping a_1 and nondropping ρ masses

We first show, in the case of nondropping ρ mass, the spectral function in the chiral limit calculated in the GHLS theory in Fig. 1 (left). Two cases are compared; one includes the V-A mixing and the other does not. The spectral function has a peak at M_ρ and a broad bump around M_{a_1} due to the mixing. The height of the spectrum at M_ρ is enhanced and a contribution above ~ 1 GeV is gone when one omits the a_1 in the calculation. One observes that a discrepancy between the two curves becomes larger above T_f where partial restoration of chiral symmetry sets in. For

finite m_π the energy of the virtual ρ meson for two processes, $\rho + \pi \rightarrow a_1$ and $\rho \rightarrow a_1 + \pi$, are split into $\sqrt{s} = M_{a_1} - m_\pi$ and $\sqrt{s} = M_{a_1} + m_\pi$. This results in the threshold effects seen as a shoulder at $\sqrt{s} = M_{a_1} - m_\pi$ and a bump above $\sqrt{s} = M_{a_1} + m_\pi$ in Fig. 1 (right). Note that the enhancement of the spectrum for $m_\pi \neq 0$ is due to the change of the phase space factor $(s - 4m_\pi^2)^{3/2}$.

In Fig. 2 we compare the vector spectrum for option A, where the a_1 bare mass changes with temperature, with that for a constant bare mass. Figure 2 (left) shows that the upper bump due to the presence of a_1 appears at lower $\sqrt{s}$ than $M_{a_1}(T = 0) = 1.26$ GeV since partial restoration of chiral symmetry sets in which makes the a_1 mass decreasing. In the case of constant a_1 mass, this bump stays at the same point as vacuum M_{a_1} at any temperature. The threshold effects for finite m_π systematically go down for the T-dependent a_1 mass and show no shift for the constant a_1 mass in Fig. 2 (right). The enhancement around $\sqrt{s} \lesssim 1$ GeV will be a signal of the partial chiral restoration.

$$T = 0.6\,T_c \text{ (below } T_f)$$

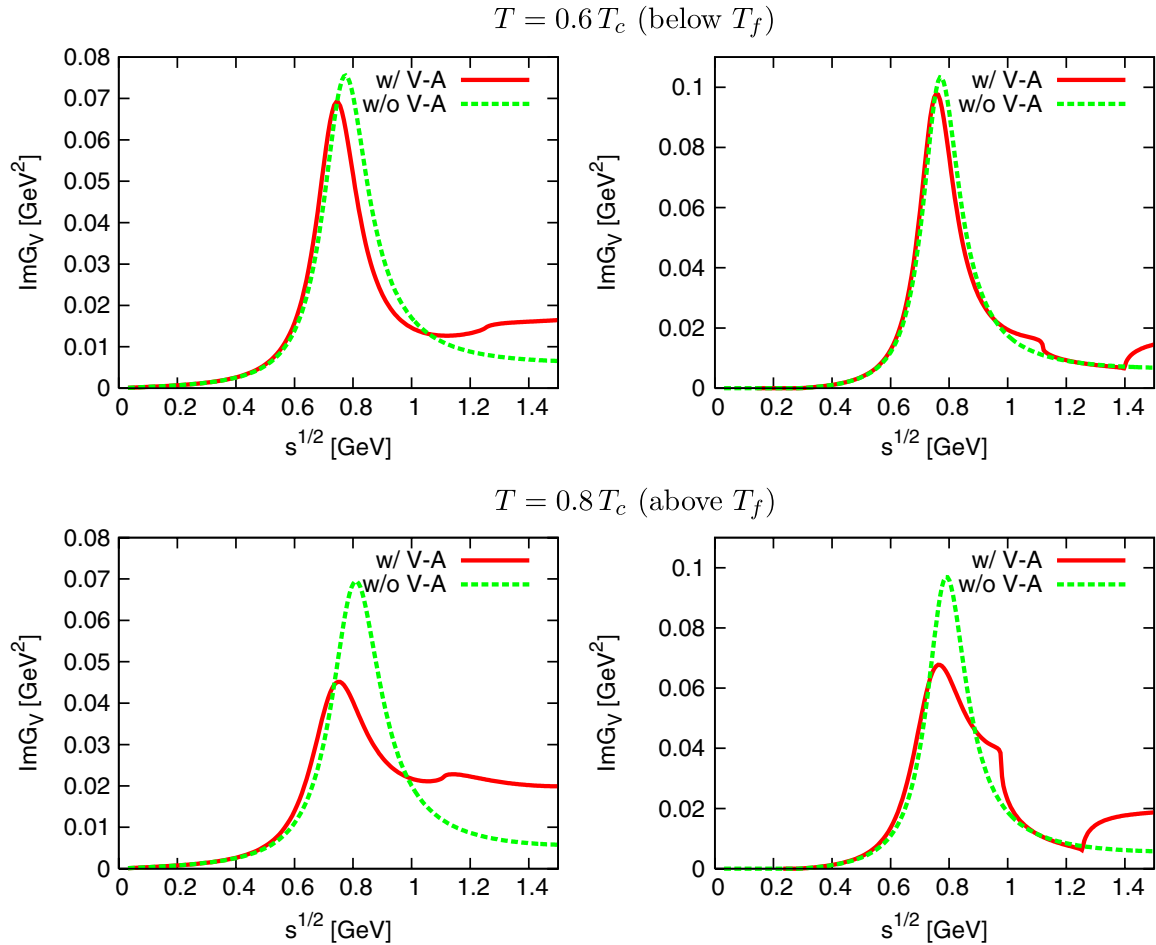$$T = 0.8\,T_c \text{ (above } T_f)$$

FIG. 1 (color online).   The vector spectral function for option A at temperature $T/T_c = 0.6$ (upper) and at $T/T_c = 0.8$ (lower) with the critical temperature $T_c = 200$ MeV, calculated in the ρ-meson rest frame. The left side figures are calculated for $m_\pi = 0$ and the right side for $m_\pi = 140$ MeV. The solid curve is obtained in the full calculation. The dashed line is calculated eliminating the axial-vector meson and hence V-A mixing from the theory.
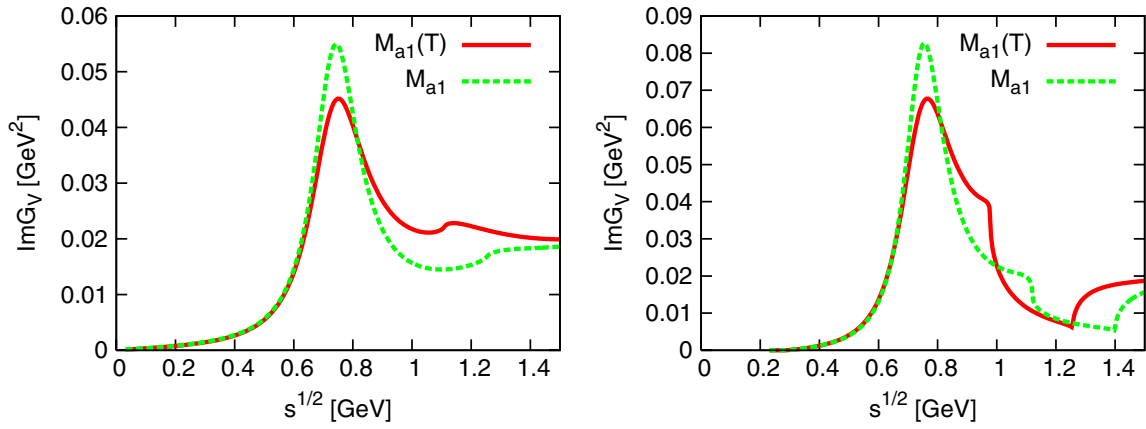
FIG. 2 (color online).   The vector spectral function at temperature $T/T_c = 0.8$ for $m_\pi = 0$ (left) and for $m_\pi = 140$ MeV (right). The solid lines are obtained for option A where the a_1 mass has a temperature dependence given in Eq. (3.3). The dashed lines are calculated for a constant a_1 mass.

Figure 3 (left) shows the temperature dependence of the vector spectral function in the chiral limit. One observes a systematic downward shift of the enhancement around the a_1 mass with temperature, while the peak position corresponding to the ρ pole mass moves upward due to the hadronic temperature corrections. At $T/T_c = 0.9$ two bumps begin to overlap: the lower one corresponds to the ρ pole, and the upper one to the a_1-π contribution. Finally at $T = T_c$, M_{a_1} becomes degenerate with M_ρ around $\sqrt{s} \simeq$ 1 GeV and the two bumps are on top of each other. Note that the V-A mixing eventually vanishes there. This feature is a direct consequence of vanishing coupling of a_1 to ρ-π, as is easily seen from Eq. (2.24). It is unchanged even if an explicit scalar field is present [20]. Figure 3 (right) shows the temperature dependence of the vector spectrum for finite m_π. Below T_c one observes the previously mentioned threshold effects moving downward with increasing temperature. It is remarkable that at T_c the spectrum shows almost no traces of a_1-ρ-π threshold effects: Eq. (3.4) together with the fact that $h_V \simeq h_A$ shows that the ρ to a_1

mass ratio becomes almost 1 at $T = T_c$:

$$\frac{M_\rho^2}{M_{a_1}^2} \xrightarrow{T \to T_c} \frac{ag^2 F^2 + h_V m_\pi^2}{ag^2 F^2 + h_A m_\pi^2} \simeq 1, \qquad (4.3)$$

and the pion decay constant is very tiny there, $F_\pi^2 \sim (h_A - h_V) m_\pi^2/g^2$. Consequently, Eq. (2.24) implies that $g_{a_1\rho\pi} \sim \sqrt{h_A - h_V} m_\pi \sim 0.06 m_\pi$. This indicates that at T_c the a_1 *meson mass nearly equals the ρ meson mass and the a_1-ρ-π coupling almost vanishes even in the presence of explicit chiral symmetry breaking.*

B. Option B: dropping a_1 and ρ masses

In case of dropping ρ and a_1 masses, the spectral function is enhanced compared to that without dropping mass since the ρ decay width is reduced [14]. Figure 4 shows the vector spectrum using the type (I) parameterization at $T = 0.8T_c$. The feature that the a_1 meson suppresses the vector spectral function through the V-A mixing remains unchanged [21]. Compared with Fig. 1 (lower-left), a bump
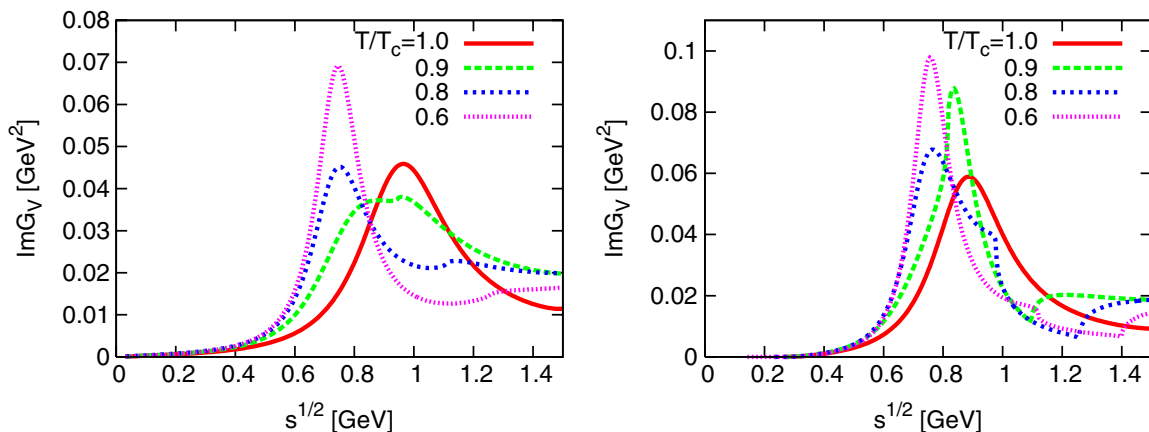

FIG. 3 (color online).   The vector spectral function (option A) for $m_\pi = 0$ (left) and for $m_\pi = 140$ MeV (right) at several temperatures $T/T_c = 0.6$–1.0.
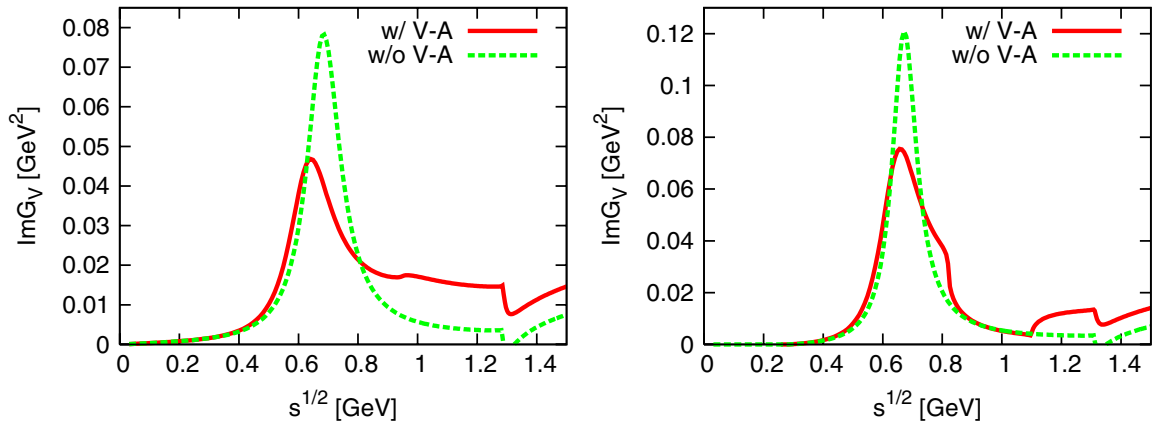
FIG. 4 (color online).   The vector spectral function (option B) for $m_\pi = 0$ (left) and for $m_\pi = 140$ MeV (right) in type (I) at temperature $T/T_c = 0.8$ with the critical temperature $T_c = 200$ MeV, calculated in the ρ-meson rest frame.

through the V-A mixing and the ρ peak are shifted downward since both the ρ and a_1 masses drop. The self-energy has a cusp at the threshold $2M_\rho$ and this appears as a dip at $\sqrt{s} \sim 1.3$ GeV. The influence of finite m_π turns out to be in threshold effects as before.

In Fig. 5 we compare type (I) with (II) at $T = 0.8T_c$. In type (II) the ρ meson mass drops faster than the a_1 mass which is clearly seen in the figure. The ρ coupling to the vector current g_ρ decreases faster than that for type (I) and this makes the spectral function somewhat suppressed compared with that for type (I).

For finite pion mass, one finds from Eqs. (3.12) and (3.13) the mass ratio near T_c

$$\frac{M_\rho^2}{M_{a_1}^2} \xrightarrow{T \to T_c} \frac{h_V}{h_A} \simeq 1, \qquad (4.4)$$

for *both* type (I) and (II). This leads to the nearly vanishing V-A mixing as seen for the nondropping ρ mass, option A [see Eq. (4.3)].

It should be noted that the vector meson becomes the chiral partner of the pion and vector-meson dominance is strongly violated when the chiral symmetry is restored in the VM [type (II)] [22]. This induces a significant reduction of the vector spectral function [14,23]. On the other hand, the pion form factor is still vector-meson dominated at T_c if the dropping ρ and a_1 join in the same chiral multiplet [type (I)] [10].

V. CONCLUSIONS

We have performed a detailed study of V-A mixing in the current correlation functions and its evolution with temperature, guided by three possible scenarios of chiral symmetry restoration: dropping ρ and a_1 masses with type (I) and (II), and alternatively dropping a_1 mass becoming degenerate with a nonzero ρ meson mass at critical temperature. In the chiral limit the axial-vector meson contributes significantly to the vector spectral function; the presence of the a_1 reduces the vector spectrum around M_ρ and enhances it around M_{a_1}. For physical pion mass
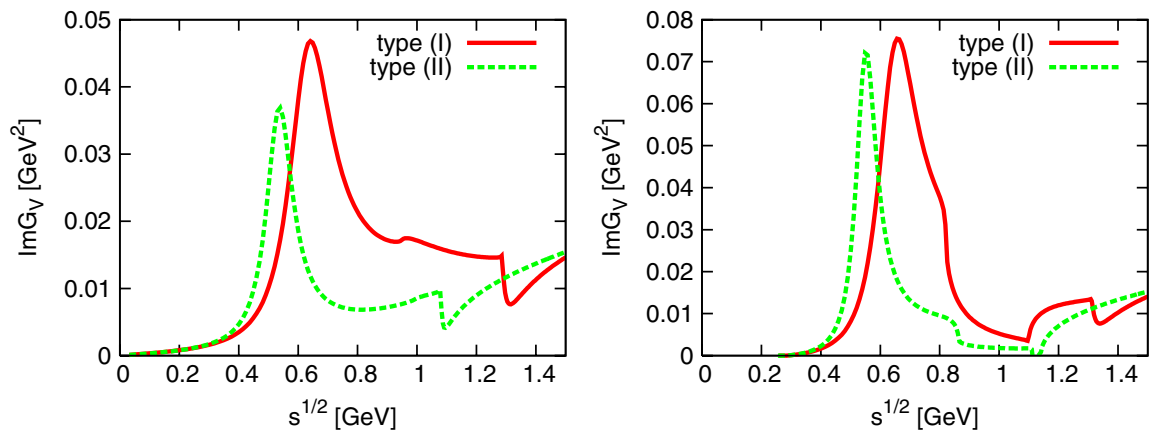

FIG. 5 (color online).   The vector spectral function (option B) for $m_\pi = 0$ (left) and for $m_\pi = 140$ MeV (right) at temperature $T/T_c = 0.8$ with the critical temperature $T_c = 200$ MeV, calculated in the ρ-meson rest frame. The solid curve is for type (I). The dashed line is for type (II).

m_π, the a_1 contribution above $\sqrt{s} \sim M_{a_1}$ still survives although the bump is somewhat reduced. A major change with both dropping ρ and a_1 masses is a systematic downward shift of the vector spectrum. We observe a different evolution of the spectrum depending on type (I) or (II) before reaching the critical temperature. The a_1-ρ-π coupling vanishes at the critical temperature T_c and thus the V-A mixing also vanishes. A remarkable observation is that even for physical m_π the ρ and a_1 meson masses are well degenerate at T_c. The vanishing V-A mixing at T_c stays almost intact.

One interesting application of this thermal spectral function is to study dilepton production in relativistic heavy-ion collisions. The change of the V-A mixing in the presence of matter and its influence on dilepton production has been evaluated based on a virial expansion for $T < m_\pi$ and $\rho < 3\rho_0$ (with normal nuclear matter density ρ_0) [24]. However, important modifications of the a_1-meson properties near critical temperature have not been treated so far in dilepton processes in the context of chiral symmetry restoration. Of course, in order to deal with dileptons realistically one needs to account for other collective excitations and many-body interactions as well as the time evolution of the created fireball [25]. Such effects can screen signals of chiral restoration [23] and make an interpretation of broad in-medium spectral functions in terms of a changing chiral order parameter quite difficult [26]. The situation at the Relativistic Heavy Ion Collider and/or the LHC might be very different from that at the Super Proton Synchrotron (SPS). At SPS energies many-body effects come from the presence of baryons. These effects are expected to be much reduced in very hot matter with relatively low baryon density. The present study may then be of some relevance for the high temperature, low baryon density scenarios encountered at the Relativistic Heavy Ion Collider and the LHC.

One caveat in the present treatment is about the lack of a genuine $\bar{q}q$ scalar meson which becomes the chiral partner of the pion in the Ginzburg-Landau picture of chiral symmetry restoration. The scalar modes are expected to be important near the chiral critical temperature and may modify the current correlators. This can be quantified by introducing explicit scalar modes in a GHLS invariant way. Work concerning the finite temperature evolution of both vector and axial-vector spectral functions in this generalized framework is in progress and will be reported elsewhere [20].

APPENDIX: TWO-POINT FUNCTIONS AT ONE LOOP

A systematic derivative expansion based on the GHLS was adopted in Ref. [10] where one finds details of its construction and quantization procedure. In the following, we list the expressions for three relevant two-point functions.

We define the Feynman integrals by

$$A_0(M) = T \sum_{n=-\infty}^{\infty} \int \frac{d^3k}{(2\pi)^3} \frac{1}{M^2 - k^2}, \qquad B_0(p; M_1, M_2) = T \sum_{n=-\infty}^{\infty} \int \frac{d^3k}{(2\pi)^3} \frac{1}{[M_1^2 - k^2][M_2^2 - (k-p)^2]},$$

$$B^{\mu\nu}(p; M_1, M_2) = T \sum_{n=-\infty}^{\infty} \int \frac{d^3k}{(2\pi)^3} \frac{(2k-p)^\mu (2k-p)^\nu}{[M_1^2 - k^2][M_2^2 - (k-p)^2]}, \tag{A1}$$

where the zeroth component of the loop momentum is taken as $k^0 = i2n\pi T$ and that of the external momentum $p^0 = i2n'\pi T$ [n, n': integer] in the standard Matsubara formalism.

The two-point function of the vector gauge field V_μ is given by

$$\Pi_V^{\mu\nu} = \int d^4x e^{ipx} \langle T V^\mu(x) V^\nu(0) \rangle$$

$$= N_f \zeta g^{\mu\nu} A_0(m_\pi) + 2N_f g^{\mu\nu} A_0(M_\rho) + N_f(\zeta^2 - 2\zeta + 3) A_0(M_{a_1}) + \frac{N_f}{8}(1+\zeta)^2 B^{\mu\nu}(p; m_\pi, m_\pi)$$

$$- N_f[M_\rho^2 g^{\mu\nu} - 4(p^2 g^{\mu\nu} - p^\mu p^\nu)] B_0(p; M_\rho, M_\rho) + \frac{9N_f}{8} B^{\mu\nu}(p; M_\rho, M_\rho)$$

$$- N_f[M_\rho^2 \zeta g^{\mu\nu} - 4(p^2 g^{\mu\nu} - p^\mu p^\nu)] B_0(p; M_{a_1}, M_{a_1}) + \frac{N_f}{8}(\zeta^2 - 4\zeta + 12) B^{\mu\nu}(p; M_{a_1}, M_{a_1})$$

$$- N_f M_\rho^2 (1-\zeta) g^{\mu\nu} B_0(p; M_{a_1}, m_\pi) + \frac{N_f}{4} \zeta(1-\zeta) B^{\mu\nu}(p; M_{a_1}, m_\pi), \tag{A2}$$

where we introduce a temperature-dependent parameter ζ as

$$\zeta(T)$$

$$= \begin{cases} \frac{M_\rho^2}{M_{a_1}^2(T)} & \text{for dropping } a_1 \text{ and non-dropping } \rho \text{ (option A)} \\ \frac{M_\rho^2(T)}{M_{a_1}^2(T)} & \text{for dropping } a_1 \text{ and } \rho: \text{type (I) or (II) (option B).} \end{cases}$$

$$(A3)$$

The relevant one-loop diagrams to the V-A mixing are shown in Fig. 6. The left diagram is proportional to $B_0(p; M_{a_1}, m_\pi)$ and the right to $B^{\mu\nu}(p; M_{a_1}, m_\pi)$. One easily finds that the V-A mixing generated from those diagrams vanishes at the critical temperature *independently of the pattern of chiral restoration*, i.e., type (I): $\zeta = 1$, type (II): $\zeta = 0$ for $M_{a_1} = M_\rho = 0$, or $\zeta = 1$ for $M_{a_1} = M_\rho \neq 0$ at T_c.
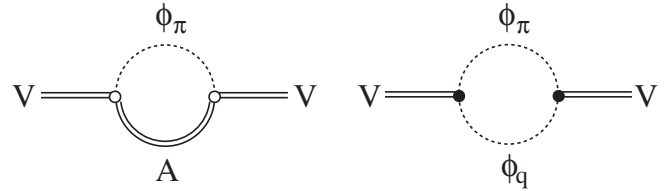

FIG. 6. Diagrams contributing to the V-A mixing at one loop. The circle ($\circ$) denotes the momentum-independent vertex and the dot ($\bullet$) denotes the momentum-dependent vertex. Vector and axial-vector fields are denoted by V and A and pion by ϕ_π. The A is the transverse components of the a_1 meson, while the ϕ_q the longitudinal one.

The two-point function of V^μ and the external vector field $\mathcal{V}^\nu$, like a photon, is found as

$$\Pi_{V\parallel}^{\mu\nu} = \int d^4x e^{ipx} \langle TV^\mu(x)\mathcal{V}^\nu(0)\rangle$$

$$= \frac{N_f}{2}(1-\zeta)g^{\mu\nu}A_0(m_\pi) + \frac{N_f}{2}g^{\mu\nu}A_0(M_\rho) + \frac{N_f}{2}\zeta g^{\mu\nu}A_0(M_{a_1}) + \frac{N_f}{8}(1-\zeta^2)B^{\mu\nu}(p; m_\pi, m_\pi)$$

$$+ N_f M_\rho^2 g^{\mu\nu}B_0(p; M_\rho, M_\rho) + \frac{N_f}{8}B^{\mu\nu}(p; M_\rho, M_\rho) + N_f M_\rho^2 \zeta g^{\mu\nu}B_0(p; M_{a_1}, M_{a_1}) + \frac{N_f}{8}(2-\zeta)B^{\mu\nu}(p; M_{a_1}, M_{a_1})$$

$$+ N_f M_\rho^2 (1-\zeta)g^{\mu\nu}B_0(p; M_{a_1}, m_\pi) - \frac{N_f}{4}\zeta(1-\zeta)B^{\mu\nu}(p; M_{a_1}, m_\pi). \tag{A4}$$

The two-point function of $\mathcal{V}^\mu$ is

$$\Pi_{\parallel}^{\mu\nu} = \int d^4x e^{ipx} \langle T\mathcal{V}^\mu(x)\mathcal{V}^\nu(0)\rangle$$

$$= \frac{N_f}{8}(1-\zeta)^2 B^{\mu\nu}(p; m_\pi, m_\pi) - \frac{N_f}{8}M_\rho^2 g^{\mu\nu}B_0(p; M_\rho, M_\rho) + \frac{N_f}{8}B^{\mu\nu}(p; M_\rho, M_\rho) - N_f M_\rho^2 \zeta B_0(p; M_{a_1}, M_{a_1})$$

$$+ \frac{N_f}{8}\zeta^2 B^{\mu\nu}(p; M_{a_1}, M_{a_1}) - N_f M_\rho^2 (1-\zeta)g^{\mu\nu}B_0(p; M_{a_1}, m_\pi) + \frac{N_f}{4}\zeta(1-\zeta)B^{\mu\nu}(p; M_{a_1}, m_\pi). \tag{A5}$$

[1] See, e.g., V. Bernard and U. G. Meissner, Nucl. Phys. **A489**, 647 (1988); T. Hatsuda and T. Kunihiro, Phys. Rep. **247**, 221 (1994); R. D. Pisarski, arXiv:hep-ph/9503330; F. Klingl, N. Kaiser, and W. Weise, Nucl. Phys. **A624**, 527 (1997); R. Rapp and J. Wambach, Adv. Nucl. Phys. **25**, 1 (2002); F. Wilczek, arXiv:hep-ph/0003183; G. E. Brown and M. Rho, Phys. Rep. **363**, 85 (2002).

[2] M. Dey, V. L. Eletsky, and B. L. Ioffe, Phys. Lett. B **252**, 620 (1990).

[3] E. Marco, R. Hofmann, and W. Weise, Phys. Lett. B **530**, 88 (2002); M. Urban, M. Buballa, and J. Wambach, Phys. Rev. Lett. **88**, 042002 (2002).

[4] See, e.g., J. Schwinger, Phys. Lett. **24B**, 473 (1967); *Paticles and Sourses* (Gordon and Greach, New York,

1969); J. Wess and B. Zumino, Phys. Rev. **163**, 1727 (1967); S. Gasiorowicz and D. A. Geffen, Rev. Mod. Phys. **41**, 531 (1969); O. Kaymakcalan, S. Rajeev, and J. Schechter, Phys. Rev. D **30**, 594 (1984).

[5] J. Gasser and H. Leutwyler, Ann. Phys. (N.Y.) **158**, 142 (1984); G. Ecker, J. Gasser, A. Pich, and E. de Rafael, Nucl. Phys. **B321**, 311 (1989).

[6] M. Bando, T. Kugo, and K. Yamawaki, Nucl. Phys. **B259**, 493 (1985); Phys. Rep. **164**, 217 (1988); M. Bando, T. Fujiwara, and K. Yamawaki, Prog. Theor. Phys. **79**, 1140 (1988).

[7] N. Kaiser and U. G. Meissner, Nucl. Phys. **A519**, 671 (1990).

[8] See, e.g., J. Schechter, Phys. Rev. D **34**, 868 (1986); K. Yamawaki, Phys. Rev. D **35**, 412 (1987); U. G. Meissner

and I. Zahed, Z. Phys. A **327**, 5 (1987); M. F. Golterman and N. D. HariDass, Nucl. Phys. **B277**, 739 (1986); G. Ecker, J. Gasser, H. Leutwyler, A. Pich, and E. de Rafael, Phys. Lett. B **223**, 425 (1989); M. Tanabashi, Phys. Lett. B **384**, 218 (1996); M. C. Birse, Z. Phys. A **355**, 231 (1996).

[9] M. Harada and K. Yamawaki, Phys. Rep. **381**, 1 (2003).

[10] M. Harada and C. Sasaki, Phys. Rev. D **73**, 036001 (2006).

[11] M. A. Shifman, A. I. Vainshtein, and V. I. Zakharov, Nucl. Phys. **B147**, 385 (1979); **B147**, 448 (1979).

[12] S. Weinberg, Phys. Rev. Lett. **18**, 507 (1967).

[13] W.-M. Yao *et al.* (Particle Data Group), J. Phys. G **33**, 1 (2006), and 2007 partial update for the 2008 edition.

[14] M. Harada and C. Sasaki, Phys. Rev. D **74**, 114006 (2006).

[15] G. E. Brown, C. H. Lee, and M. Rho, Nucl. Phys. **A747**, 530 (2005).

[16] M. Harada and C. Sasaki, Phys. Lett. B **537**, 280 (2002).

[17] M. Cheng *et al.*, Phys. Rev. D **77**, 014511 (2008).

[18] G. E. Brown and M. Rho, Phys. Rev. Lett. **66**, 2720 (1991).

[19] M. Harada and C. Sasaki, Nucl. Phys. **A736**, 300 (2004).

[20] M. Harada, C. Sasaki, and W. Weise (unpublished).

[21] C. Sasaki, M. Harada, and W. Weise, arXiv:0805.4792.

[22] M. Harada and K. Yamawaki, Phys. Rev. Lett. **86**, 757 (2001).

[23] G. E. Brown, M. Harada, J. W. Holt, M. Rho, and C. Sasaki, arXiv:0804.3196.

[24] J. V. Steele, H. Yamagishi, and I. Zahed, Phys. Lett. B **384**, 255 (1996); Phys. Rev. D **56**, 5605 (1997); K. Dusling, D. Teaney, and I. Zahed, Phys. Rev. C **75**, 024908 (2007); K. Dusling and I. Zahed, arXiv:0712.1982.

[25] H. van Hees and R. Rapp, arXiv:hep-ph/0604269; Nucl. Phys. **A806**, 339 (2008); J. Ruppert and T. Renk, Eur. Phys. J. C **49**, 219 (2007); R. Rapp, J. Phys. G **34**, S405 (2007); H. van Hees, J. Phys. G **35**, 104034 (2008).

[26] Y. Kwon, M. Procura, and W. Weise, arXiv:0803.3262 [Phys. Rev. C (to be published)].